Optimal Nonlinear Feedack Control for Spacecraft Attitude Maneuvers

C.K. Carrington* and J.L. Junkins†
Virginia Polytechnic Institute and State University, Blacksburg, Virginia

Polynomial feedback controls for large-angle, nonlinear spacecraft attitude maneuvers are developed. A five-body configuration consisting of an asymmetric spacecraft and four reaction wheels is considered. Attention is restricted to the momentum transfer class of internal control torques; this, in conjunction with the choice of Euler parameters as attitude coordinates, permits several important order reduction simplifications. Three numerical examples are included to illustrate applications of the concepts presented.

Introduction

RAPID large-angle attitude maneuvers have become increasingly important to the success of many current and future spacecraft missions. These maneuvers are characterized by nonlinear behavior, however, resulting in a control problem that is likewise nonlinear. One approach to feedback control of nonlinear motion is "gain scheduling" in which the control history is divided into segments, each determined by its own set of linear gains. A more attractive approach is control of the entire nonlinear maneuver by a single set of gains.

For the latter approach, a method is presented whereby the optimal nonlinear control problem is solved in polynomial feedback form and a suboptimal control law is determined by truncation. Currently there are two approaches used to determine the polynomial coefficients for the control. One is to expand the coast-to-go functional as a polynomial in the states and then recursively solve the Hamilton-Jacobi-Bellman equation, as discussed by Willenstein,[1] Dabbous and Ahmed,[2] and Dwyer and Sena.[3] In the method used here,[4] the control itself is expanded as a polynomial and the coefficients determined recursively from the costate equations.

General Formulation

Polynomial state equations may be written in indicial notation as

$$\dot{x}_i = a_{ij}x_j + c_{ijk}x_jx_k + \dots + b_{ij}u_j \qquad (i=1,2,\dots,n) \qquad (1)$$

where x_i are the states and u_i the controls to be determined. Consider the optimal control problem of finding a feedback control law that brings the states to zero while minimizing a quadratic performance index

$$J = \frac{1}{2}\int_{t_0}^{t_f} \{q_{ij}x_ix_j + r_{ij}u_iu_j\}\,dt \qquad (2)$$

The Hamiltonian for this system is

$$\mathcal{H} = ½\{q_{ij}x_ix_j + r_{ij}u_iu_j\} + \lambda_i\dot{x}_i \qquad (3)$$

where it is understood that $\dot{x}_i$ is symbolic for the right-hand side of Eq. (1). The necessary conditions for a minimum provide the state equation, Eq. (1),

$$\dot{x}_i = \frac{\partial\mathcal{H}}{\partial\lambda_i} \qquad (4)$$

and the costate equation

$$\dot{\lambda}_i = -\frac{\partial\mathcal{H}}{\partial x_i} \qquad (5)$$

For unbounded control

$$\frac{\partial\mathcal{H}}{\partial u_i} = 0 \qquad (6)$$

which implies

$$u_i = -r_{ij}^{-1}b_{kj}\lambda_k \qquad (7)$$

where r_{ij}^{-1} represents the elements of the matrix inverse of r_{ij}. By assuming the costates can be expressed as a polynomial in the states, as in Ref. 4,

$$\lambda_i = k_{ij}x_j + d_{ijk}x_jx_k + \dots \qquad (8)$$

a nonlinear feedback control law is determined in which $k_{ij}(t)$ and $d_{ijk}(t)$ are the control gains sought. By substituting Eq. (8) into Eq. (5) and carrying out the ensuing algebra, we are led to n homogeneous polynomial equations of the form

$$[\alpha]x_j + [\beta]x_jx_k + \dots = 0 \qquad (9)$$

where

$$[\alpha] = \text{function } (A,B,Q,R,\dot{K},K)$$

$$[\beta] = \text{function } (A,B,C,R,K,\dot{D},D)$$

and K and D are arrays whose elements are the gains k_{ij} and d_{ijk}. Since Eq. (9) must hold at every point in the state space, it is concluded that the functions in brackets must vanish in-

Presented as Paper 83-2230 at the AIAA Guidance and Control Conference, Gatlinburg, TN, Aug. 15-17, 1983; submitted Sept. 30, 1983; revision submitted June 18, 1985.

*Graduate Research Assistant; presently Assistant Professor of Mechanical Engineering, University of South Carolina, Columbia, SC. Student Member AIAA.

†Professor, Engineering Science and Mechanics. Associate Fellow AIAA.

dependently, so we obtain

$$[\alpha(A,B,Q,R,\dot{K},K)]=0 \tag{10}$$

$$[\beta(A,B,C,R,K,\dot{D},D)]=0 \tag{11}$$

Equation (10) is a matrix differential equation determining the linear feedback gains; upon carrying through the details, we find that the scalar equations of Eq. (10) are precisely the elements of the matrix Riccati equation which generates the optimal feedback control if all nonlinear terms in the state equation are absent. The solution for the matrix Riccati equation can be determined by Potter[5] or Turner's[6] method, in which an associated eigenvalue problem is solved and matrix exponentials are used.

The quadratic feedback gains are determined by Eq. (11), which can be rearranged into a set of linear differential equations of the form

$$\dot{d}_{ijk}=[\eta]d_{\ell mr}+[\gamma] \tag{12}$$

where

$$\begin{aligned}[\eta]&=\text{function }(A,B,C,R,K)\\ [\gamma]&=\text{function }(A,B,C,R,K)\end{aligned} \tag{13}$$

Upon solving the Riccati eqaution for the linear gains $k_{\ell m}(t)$, Eq. (12) provides nonautonomous, nonhomogeneous, but linear equations that determine the quadratic gains $d_{ijk}(t)$. For the steady-state case, Eqs. (10) and (11) can be solved algebraically for the constant feedback gains subject to

$$\dot{k}_{\ell m}=\dot{d}_{\ell mk}=0 \tag{14}$$

The $k_{\ell m}$ are solutions of the algebraic Riccati equation, and the $d_{\ell mr}$ are obtained by setting $\dot{d}_{ijk}=0$ in Eq. (12) and inverting the linear algebraic system. In the numerical examples considered herein, attention is restricted to the constant gain case.

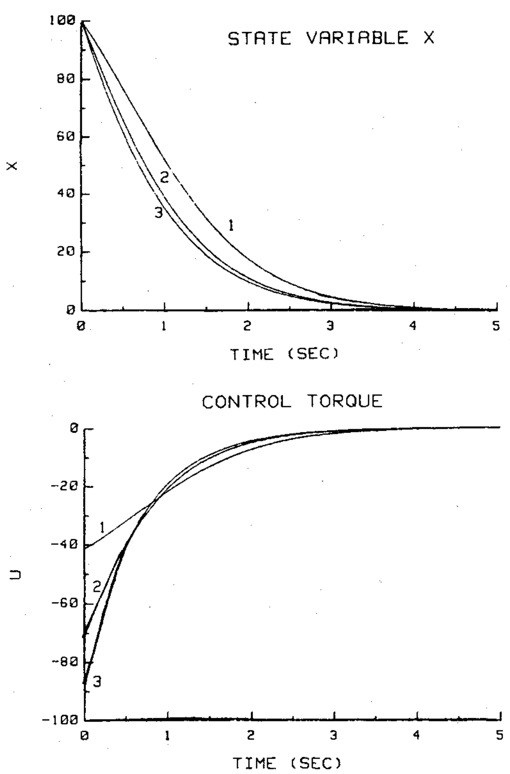

Fig. 1 Scalar example: 1, linear feedback; 2, linear plus quadratic feedback; 3, linear through cubic feedback.

Since for n states there are $n^2(n+1)/2$ equations in Eq. (12), we do not include the algebra of the system considered here. The emphasis of this discussion is the following generalization: After solving the Riccati equation for the linear gains, one is led to sets of linear differential equations, of the functional form shown in Eq. (12), that can be solved sequentially to obtain the quadratic gains, the cubic gains, and so on, up to any desired order. The differential equations for the gains of each order depend upon the lower order gains.

Scalar Example

Consider the optimal control problem of minimizing the following performance index:

$$J=\frac{1}{2}\int_{t_0}^{t_f}\{x^2+u^2\}\mathrm{d}t \tag{15}$$

subject ot the state equation

$$\dot{x}=-x+\epsilon x^2+u \tag{16}$$

The costate equation is

$$\dot{\lambda}=-x+\lambda-2\epsilon\lambda x \tag{17}$$

and the control is

$$u=-\lambda \tag{18}$$

Table 1 Scalar example performance indices

Feedback order	Performance index
1	4314.8
2	3796.4
3	3725.5
4	3717.2
5	3716.8

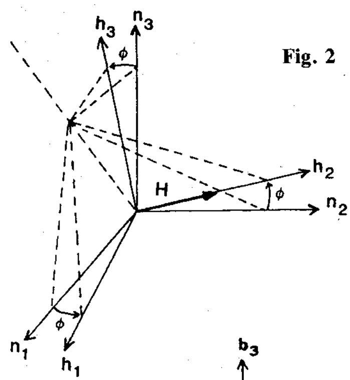

Fig. 2 Momentum reference frame.

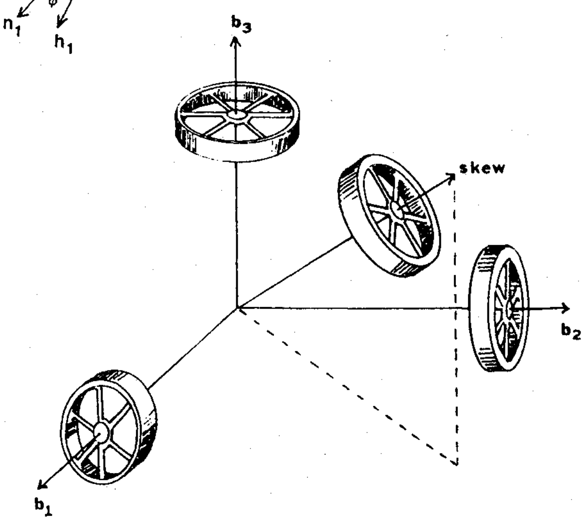

Fig. 3 NASA standard four reaction wheel attitude control system.

Assuming the costate as a polynomial in state x,

$$\lambda = k_1 x + k_2 x^2 + k_3 x^3 + \dots \tag{19}$$

then the coefficient differential equations corresponding to Eqs. (10) and (11) and higher order terms are

$$\dot{k}_1 - 2k_1 + 1 - k_1^2 = 0$$

$$\dot{k}_2 - 3(k_1+1)k_2 = -3k_1\epsilon$$

$$\dot{k}_3 - 4(k_1+1)k_3 = 2k_2^2 - 4k_2\epsilon$$

$$\dot{k}_4 - 5(k_1+1)k_4 = 5k_2k_3 - 5k_3\epsilon$$

$$\dot{k}_5 - 6(k_1+1)k_5 = 6k_2k_4 + 3k_3^2 - 6k_4\epsilon$$

$$\vdots$$

$$\dot{k}_n - (n+1)(k_1+1)k_n = (n+1)\{k_2k_{n-1} + k_3k_{n-2} + \dots + k_{n/2}k_{n/2+1} - k_{n-1}\epsilon\} \text{ for } n \text{ even}$$

$$\dot{k}_n - (n+1)(k_1+1)k_n = (n+1)\{k_2k_{n-1} + k_3k_{n-2} + \dots + k_{(n-1)/2}k_{(n+3)/2} + \tfrac{1}{2}k_{(n+1)/2}^2 - k_{n-1}\epsilon\} \text{ for } n \text{ odd} \tag{20}$$

Making the change of variable from time t to time-to-go $\tau = t_f - t$ and assuming a solution of the form

$$k_1 = k_{1SS} + z_1^{-1}$$

$$k_2 = z_1^{-3}z_2$$

$$k_3 = z_1^{-4}z_3$$

$$\vdots$$

$$k_n = z_1^{-(n+1)}z_n \tag{21}$$

where k_{1SS} is the steady-state solution for k_1, we obtain the following equations:

$$\frac{dz_1}{d\tau} - 2(1+k_{1SS})z_1 - 1 = 0$$

$$\frac{dz_2}{d\tau} - 3(1+k_{1SS})z_2 = 3(k_{1SS}z_1^3 + z_1^2)\epsilon$$

$$\frac{dz_3}{d\tau} - 4(1+k_{1SS})z_3 = 4z_1z_2\epsilon - 2z_1^{-2}z_2^2$$

$$\vdots$$

$$\frac{dz_n}{d\tau} - (n+1)(1+k_{1SS})z_n = (n+1)\{z_1z_{n-1}\epsilon - z_1^{-2}(z_2z_{n-1} + z_3z_{n-2} + \dots + z_{(n/2+1)})\} \text{ for } n \text{ even}$$

$$\frac{dz_n}{d\tau} - (n+1)(1+k_{1SS})z_n = (n+1)\{z_1z_{n-1}\epsilon - z_1^{-2}(z_2z_{n-1} + z_3z_{n-2} + \dots + z_{(n-1)/2}z_{(n+3)/2} + \tfrac{1}{2}z_{(n+1)/2}^2)\} \text{ for } n \text{ odd} \tag{22}$$

The variable changes of Eqs. (21) are generalizations of and were motivated by Refs. 6 and 7.

Equations (22) are easily solved, subject to specification of the boundary conditions; e.g., $k_1(\tau) = \dots = k_2(\tau) = 0$ at $\tau = 0$. Substitution of the solution for $z_i(\tau)$ into Eqs. (21) and then Eq. (19) yields a polynomial feedback control law with time-dependent coefficients.

A numerical example for the scalar case is included, using $\epsilon = 0.01$ and $t_f = 5$ s. The performance indices are given in Table 1, and the state variable and control histories are given in Fig. 1. Curves corresponding to fourth- and fifth-order feedback are coincident with third order and, hence, are not plotted. Fifth-order polynomial feedback essentially has converged to the optimal control for this scalar problem.

A system for attitude control of a spacecraft with four reaction wheels is now examined.

Spacecraft Orientation

Euler Parameters

A spacecraft body-fixed reference frame $\{\hat{b}\}$ is related to an inertial frame $\{\hat{n}\}$ by the direction cosine matrix $[C(\beta)]$,

$$\{\hat{b}\} = [C(\beta)]\{\hat{n}\} \tag{23}$$

where $[C(\beta)]$ is defined in terms of the four Euler parameters $(\beta_0, \beta_1, \beta_2, \beta_3)$.[8] These attitude variables are related to the body-frame components of the spacecraft angular velocity ω by the following kinematic differential equations:

$$\dot{\beta}_0 = -\tfrac{1}{2}(\beta_1\omega_1 + \beta_2\omega_2 + \beta_3\omega_3), \quad \dot{\beta}_1 = \tfrac{1}{2}(\beta_0\omega_1 - \beta_3\omega_2 + \beta_2\omega_3)$$

$$\dot{\beta}_2 = \tfrac{1}{2}(\beta_3\omega_1 + \beta_0\omega_2 - \beta_1\omega_3), \quad \dot{\beta}_3 = -\tfrac{1}{2}(\beta_2\omega_1 - \beta_1\omega_2 - \beta_0\omega_3) \tag{24}$$

with

$$(\dot{\cdot}) \equiv \frac{d}{dt}(\ )$$

Momentum Reference Frame

In addition to using an arbitrary, general inertial frame $\{\hat{n}\}$, a special inertial angular momentum frame $\{\hat{h}\}$ is introduced where $\hat{h}_2$ is aligned with the system angular momentum H, as discussed by Vadali and Junkins[9] and Kraige and Junkins.[10] The other two unit vectors can be defined by the directions $\hat{n}_1$ and $\hat{n}_3$ assume after $\hat{n}_2$ is rotated to coincide with H (see Fig. 2). This reference frame can be considered inertial if the external torques are negligible during the maneuver and only internal torques are present. As is shown below, introducing this frame allows a use of the angular momentum integral to reduce the number of state variables.

The orientation of $\{\hat{b}\}$ with respect to the momentum frame $\{\hat{h}\}$ is given by the projection

$$\{\hat{b}\} = [C(\delta)]\{\hat{h}\} \tag{25}$$

where the 3×3 direction cosine matrix $[C]$ is a function of four variable Euler parameters $(\delta_0, \delta_1, \delta_2, \delta_3)$. The inertial frame $\{\hat{n}\}$ is projected onto $\{\hat{h}\}$ by

$$\{\hat{n}\} = [C(\alpha)]\{\hat{h}\} \tag{26}$$

where $(\alpha_0, \alpha_1, \alpha_2, \alpha_3)$ are constant Euler parameters since both $\{\hat{n}\}$ and $\{\hat{h}\}$ are inertial. Using the inertial frame $\{\hat{n}\}$ components of the system angular momentum

$$H = H_{n1}\hat{n}_1 + H_{n2}\hat{n}_2 + H_{n3}\hat{n}_3 \tag{27}$$

the constant α_i Euler parameters can be defined as

$$\alpha_0 = \left[\frac{H + H_{n2}}{2H}\right]^{1/2}$$

$$\alpha_1 = -H_{n3}\left[\frac{H - H_{n2}}{2H(H_{n1}^2 + H_{n3}^2)}\right]^{1/2}$$

$$\alpha_2 = 0$$

$$\alpha_3 = H_{n1}\left[\frac{H-H_{n2}}{2H(H_{n1}^2+H_{n3}^2)}\right]^{1/2} \tag{28}$$

The δ_i Euler parameters are then related to the α_i parameters by the bilinear, orthogonal equation

$$\begin{Bmatrix}\delta_0\\ \delta_1\\ \delta_2\\ \delta_3\end{Bmatrix} = \begin{bmatrix}\alpha_0 & -\alpha_1 & -\alpha_2 & -\alpha_3\\ \alpha_1 & \alpha_0 & -\alpha_3 & \alpha_2\\ \alpha_2 & \alpha_3 & \alpha_0 & -\alpha_1\\ \alpha_3 & -\alpha_2 & \alpha_1 & \alpha_0\end{bmatrix}\begin{Bmatrix}\beta_0\\ \beta_1\\ \beta_2\\ \beta_3\end{Bmatrix} \tag{29}$$

and are related to the body-frame components of ω by the differential equations

$$\dot{\delta}_0 = -\tfrac{1}{2}(\delta_1\omega_1 + \delta_2\omega_2 + \delta_3\omega_3)$$

$$\dot{\delta}_1 = \tfrac{1}{2}(\delta_0\omega_1 - \delta_3\omega_2 + \delta_2\omega_3)$$

$$\dot{\delta}_2 = \tfrac{1}{2}(\delta_3\omega_1 + \delta_0\omega_2 - \delta_1\omega_3)$$

$$\dot{\delta}_3 = -\tfrac{1}{2}(\delta_2\omega_1 - \delta_1\omega_2 - \delta_0\omega_3) \tag{30}$$

It can be shown from Eq. (25) and using the algebraic expressions for $[c(\delta)]$ from Ref. 8 or 10 that

$$\hat{h}_2 = 2(\delta_1\delta_2 + \delta_0\delta_3)\hat{b}_1 + (\delta_0^2 - \delta_1^2 + \delta_2^2 - \delta_3^2)\hat{b}_2 + 2(\delta_2\delta_3 - \delta_0\delta_1)\hat{b}_3 \tag{31}$$

so the body-frame components of the system angular momentum can now be written from $H = H\hat{h}_2$ as

$$H_1 = 2(\delta_1\delta_2 + \delta_0\delta_3)H$$

$$H_2 = (\delta_0^2 - \delta_1^2 + \delta_2^2 - \delta_3^2)H$$

$$H_3 = 2(\delta_2\delta_3 - \delta_0\delta_1)H \tag{32}$$

Thus we have an explicit relationship to eliminate H_i in terms of δ_i.

Spacecraft and Reaction Wheel Dynamics

An arbitrary asymmetric spacecraft with four reaction wheels in NASA standard configuration is considered (see Fig. 3). The system angular momentum $\boldsymbol{H}$ is the sum of the spacecraft and wheel angular momenta; the body components of $\boldsymbol{H}$ and ω are related by

$$\boldsymbol{H} = [I^*]\omega + [\tilde{C}]^T[J]\boldsymbol{\Omega} \tag{33}$$

where $[I^*]$ is the system inertia matrix with respect to the body frame $\{\hat{b}\}$, $\boldsymbol{\Omega}$ a vector of the four-wheel angular velocities, and $[J]$ the wheel axial moment of inertia matrix defined by $[J] = \text{diag}\{J_{ai}\}$, $i = 1,2,3,4$. $[\tilde{C}]$ is a 4×3 matrix whose rows are the three orthogonal body-frame components of four unit vectors along the wheel spin axes.

Assuming negligible external torques, the time rate of change of the angular momentum is zero, and thus the Eulerian equation of motion is obtained

$$\dot{\boldsymbol{H}} = [I^*]\dot{\omega} + [\tilde{C}]^T[J]\dot{\boldsymbol{\Omega}} + [\tilde{\omega}]\boldsymbol{H} = 0 \tag{34}$$

where

$$[\tilde{\omega}] = \begin{bmatrix}0 & -\omega_3 & \omega_2\\ \omega_3 & 0 & -\omega_1\\ -\omega_2 & \omega_1 & 0\end{bmatrix} \tag{35}$$

The reaction wheel equations of motion are

$$[J]\dot{\boldsymbol{\Omega}} + [J][\tilde{C}]\dot{\omega} = \boldsymbol{u} \tag{36}$$

where the four components of the control vector $\boldsymbol{u}$ are the axial torques applied to their respective wheels by the motors. To eliminate the wheel angular velocities $\boldsymbol{\Omega}$ from the spacecraft equations of motion, Eq. (36) is multiplied by $[\tilde{C}]^T$ and then substituted into Eq. (34) to obtain

$$\dot{\omega} = -[G]\{[\tilde{\omega}]\boldsymbol{H} + [\tilde{C}]^T\boldsymbol{u}\} \tag{37}$$

where $[G] = [I^* - \tilde{C}^T J\tilde{C}]^{-1}$, a constant matrix. Implicit in Eq. (37) is the substitution of Eqs. (32); thus, $\dot{\omega} = f(\omega,\delta,\boldsymbol{u})$. Notice the pleasing truth that rest-to-rest maneuvers (characterized by $\boldsymbol{H} = 0$) remove all of the gyroscopic terms in Eq. (37). It is evident that, for this class of maneuvers, angular velocity control is near trivial and attitude control is nonlinear only because of kinematic nonlinearities.

The three equations of motion in Eq. (37) and the four attitude equations in Eq. (30) will be used to determine the state equations.

Optimal Feedback Control Formulation

State Equations

To obtain state equations of the form

$$\dot{x} = Ax + F(x) + Bu \tag{38}$$

in which A is a constant coefficient matrix and $F(x)$ a vector function containing the nonlinear terms, let the state variables be the spacecraft angular velocities ω_i and Euler parameter differences $\tilde{\delta}_i$; thus, the seven-element state vector is

$$x = \{\omega_1\ \omega_2\ \omega_3\ \tilde{\delta}_0\ \tilde{\delta}_1\ \tilde{\delta}_2\ \tilde{\delta}_3\}^T \tag{39}$$

where

$$\tilde{\delta}_i = \delta_i - \delta_i(t_f) \qquad (i = 0,1,2,3) \tag{40}$$

These new state variables introduce linear terms into the dynamic and kinematic equations, Eqs. (37) and (30), respectively.

The elements of the A matrix for the linear part of the state equations are found to be

$$a_{11} = g_{12}H_3^0 - g_{13}H_2^0 \qquad a_{12} = g_{13}H_1^0 - g_{11}H_3^0$$

$$a_{13} = g_{11}H_2^0 - g_{12}H_1^0 \qquad a_{21} = g_{22}H_3^0 - g_{23}H_2^0$$

$$a_{22} = g_{23}H_3^0 - g_{21}H_3^0 \qquad a_{23} = g_{21}H_2^0 - g_{22}H_1^0$$

$$a_{31} = g_{32}H_3^0 - g_{33}H_2^0 \qquad a_{32} = g_{23}H_1^0 - g_{31}H_3^0$$

$$a_{33} = g_{31}H_2^0 - g_{32}H_1^0 \qquad a_{41} = -\delta_1(t_f)/2$$

$$a_{42} = -\delta_2(t_f)/2 \qquad a_{43} = -\delta_3(t_f)/2$$

$$a_{51} = \delta_0(t_f)/2 \qquad a_{52} = -\delta_3(t_f)/2$$

$$a_{53} = \delta_2(t_f)/2 \qquad a_{61} = \delta_3(t_f)/2$$

$$a_{62} = \delta_0(t_f)/2 \qquad a_{63} = -\delta_1(t_f)/2$$

$$a_{71} = -\delta_2(t_f)/2 \qquad a_{72} = \delta_1(t_f)/2$$

$$a_{73} = \delta_0(t_f)/2$$

$$a_{ij} = 0\,(i = 1,\ldots,7; \qquad j = 4,\ldots,7) \tag{41}$$

where $\boldsymbol{H}^0$ is Eq. (32) evaluated at $\delta_i(t_f)$ and g_{ij} are the elements of matrix $[G]$ defined after Eq. (37). Notice that a_{ij}

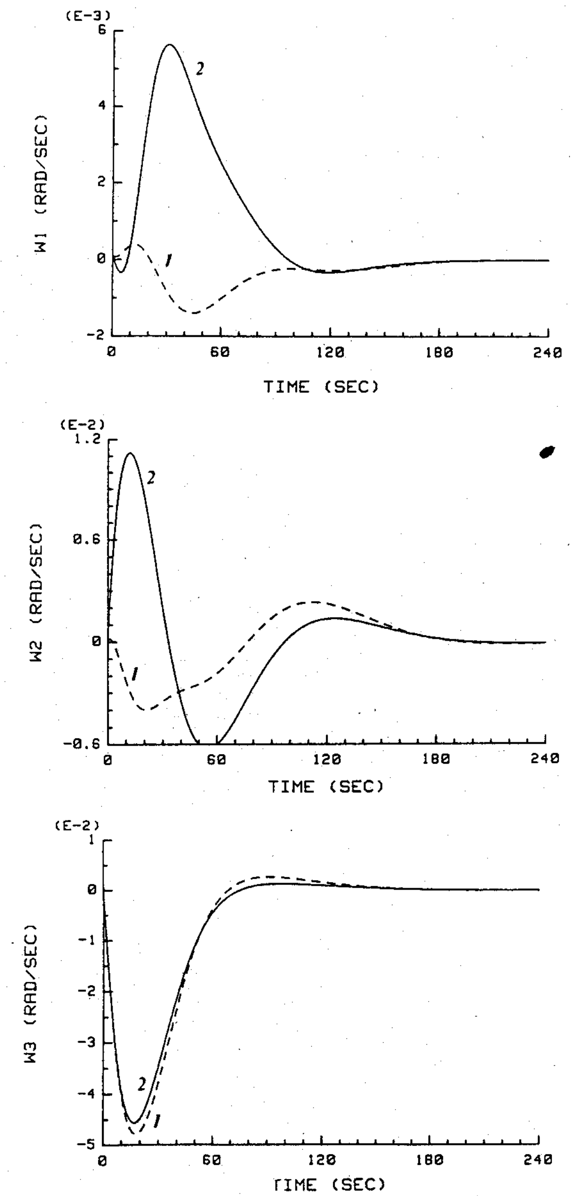

Fig. 4 Case 1: Spacecraft angular velocities.

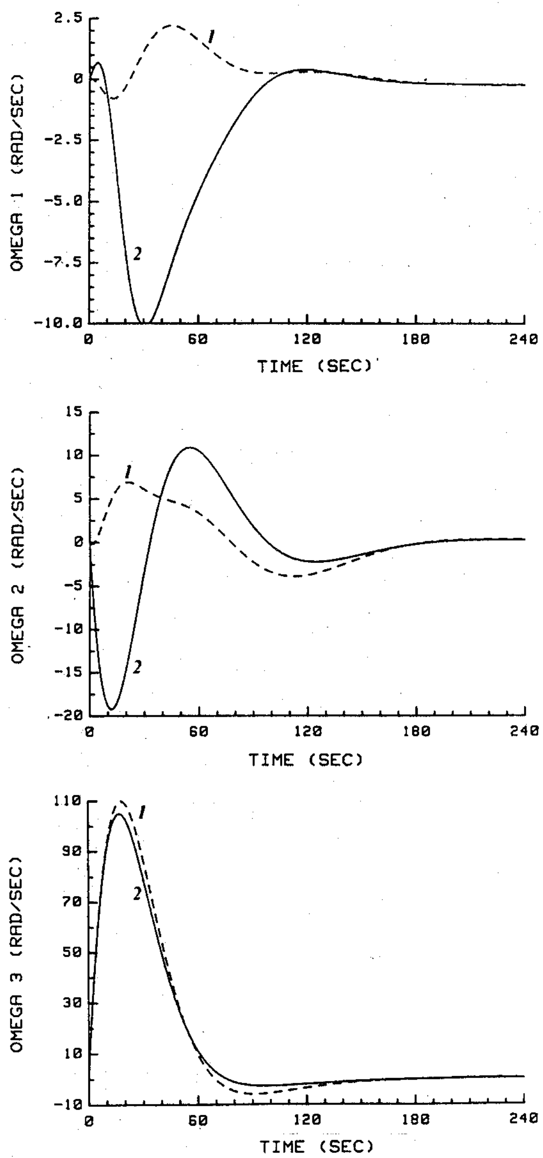

Fig. 5 Case 1: Wheel angular velocities: 1, linear feedback; 2, linear plus quadratic feedback.

are explicit functions of the specific terminal state $\delta_i(t_f)$ and the magnitude of the system angular momentum H. B is a 7×4 matrix

$$B=\begin{bmatrix} -[G][\tilde{C}]^T \\ \hdashline 0 \end{bmatrix} \tag{42}$$

and the vector $F(x)$ contains quadratic and cubic terms in x_i.

Performance Index

Two quadratic performance indices are considered

$$J_1=\frac{1}{2}\int_{t_0}^{t_f}\{x^TQx+u^TRu\}\mathrm{d}t \tag{43}$$

and

$$J_2=\frac{1}{2}\int_{t_0}^{t_f}\{x^TQx+m^TWm\}\mathrm{d}t \tag{44}$$

where

$$m=[\tilde{C}]^Tu \tag{45}$$

is a 3×1 vector containing the orthogonal components of the vector sum of the motor torques. J_1 penalizes the four motor torques and J_2 penalizes their projections on the principal axes.

In the numerical examples, performance index J_1 is used for maneuvers involving all four wheels. Performance index J_2 may also be used with four wheels, but the wheel torques are not unique, as shown below. All examples utilizing three wheels use J_2, in which the 4×3 matrix $[\tilde{C}]$ in Eq. (45) is replaced by its 3×3 nonzero submatrix. Q is a positive semidefinite weighting matrix, and R and W are identity matrices for the examples considered.

Feedback Control

For the performance index in Eq. (43), the optimal control is

$$u=-R^{-1}B_1^T\lambda \tag{46}$$

where B_1 is the B matrix of Eq. (42). The analogous development for the performance index of Eq. (44) uses the state equations in the form

$$\dot{x}=Ax+F(x)+B_2m \tag{47}$$

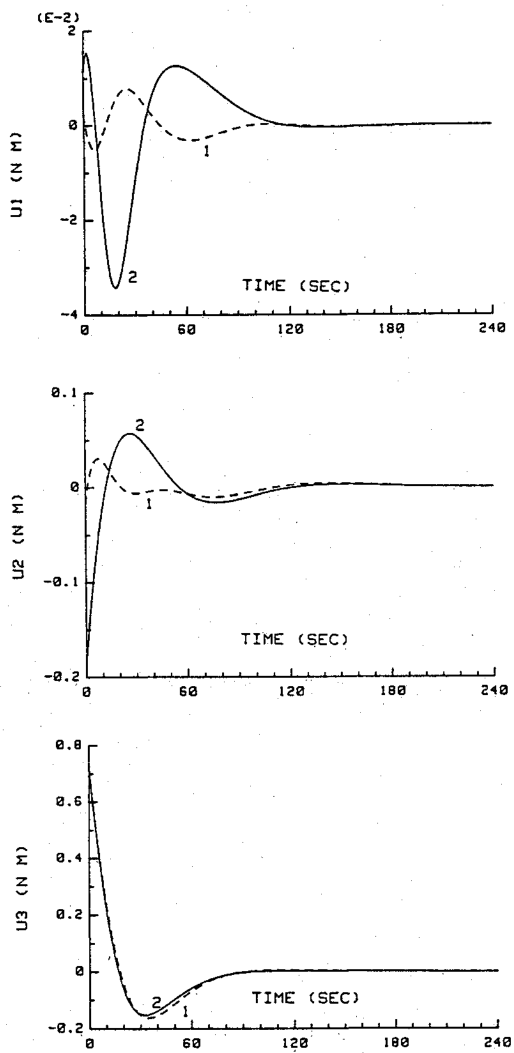

Fig. 6 Case 1: Control torques.

where B_2 is a 7×3 matrix

$$B_2 = \left[\begin{array}{c} -[G] \\ \hdashline 0 \end{array} \right] \tag{48}$$

The optimal control m for J_2 is

$$m = -W^{-1} B_2^T \lambda \tag{49}$$

and the wheel torques u are obtained by inverting Eq. (45). This solution for u is not unique unless $[\tilde{C}]$ is a square matrix.

Numerical Examples

Several examples are considered for an asymmetric spacecraft with four reaction wheels, as shown in Fig. 3. The moments of inertia of the spacecraft without the wheels and the wheel axial moment of inertia are given in Table 2; the inertia matrix $[I^*]$ and the wheel geometry matrix $[\tilde{C}]$ are given in Table 3. All examples were performed using linear and quadratic steady-state gains with free final time t_f. The examples start with zero initial conditions for wheel and spacecraft velocities and end with large initial conditions.

Case 1

A four-wheel maneuver using J_1 and several three-wheel maneuvers using J_2 are executed, all with zero initial wheel speeds. Boundary conditions are given in Table 4 using the 3-1-3 Euler angles. Table 5 contains the performance indices,

Table 2 Moments of inertia, kg-m²

I_1	86.215
I_2	85.070
I_3	113.565
J_a	0.05

Table 3 Inertia and wheel geometry matrices

$$[I^*] = \begin{bmatrix} 87.212 & -0.2237 & -0.2237 \\ -0.2237 & 86.067 & -0.2237 \\ -0.2237 & -0.2237 & 114.562 \end{bmatrix}$$

$$[\tilde{C}] = \begin{bmatrix} 1 & 0 & 0 \\ 0 & 1 & 0 \\ 0 & 0 & 1 \\ \sqrt{3}/3 & \sqrt{3}/3 & \sqrt{3}/3 \end{bmatrix}$$

Table 4 Case 1: Boundary conditions

	Initial states	Final states
ω_1	0.0001	0.0
ω_2	0.0001	0.0
ω_3	0.0001	0.0
ϕ	$-\pi/2$	$\pi/2$
θ	$-\pi/3$	$\pi/3$
φ	$-\pi/4$	$\pi/4$
δ_0	−0.54611	−0.30257
δ_1	0.47921	−0.13976
δ_2	0.67687	0.81747
δ_3	0.11820	046974
β_0	−0.33141	0.33141
β_1	0.46194	0.46194
β_2	−0.19134	0.19134
β_3	0.80010	0.80010
Ω_1	0.0	—[a]
Ω_2	0.0	—[a]
Ω_3	0.0	—[a]
Ω_4	0.0	—[a]

[a]Specific final boundary conditions for $\Omega_i(t_f)$ need not be formally enforced; these are determined implicitly because angular momentum is conserved; i.e., for H=const and $\omega(t_f)$ specified, $\Omega(t_f)$ is implicitly constrained by Eq. (33).

Table 5 Case 1: Performance indices

	Linear feedback	Linear plus quadratic feedback
Four wheels, J_1		
Q_1	6.15126	6.13691
Q_2	5.76886	5.62314
Skew wheel off, J_2		
Q_1	6.48600	6.47143
Q_2	5.92983	5.73828
Third wheel off, J_2		
Q_2	5.93077	5.76176
Second wheel off, J_2		
Q_2	5.92980	5.76077
First wheel off, J_2		
Q_2	5.92962	5.76071

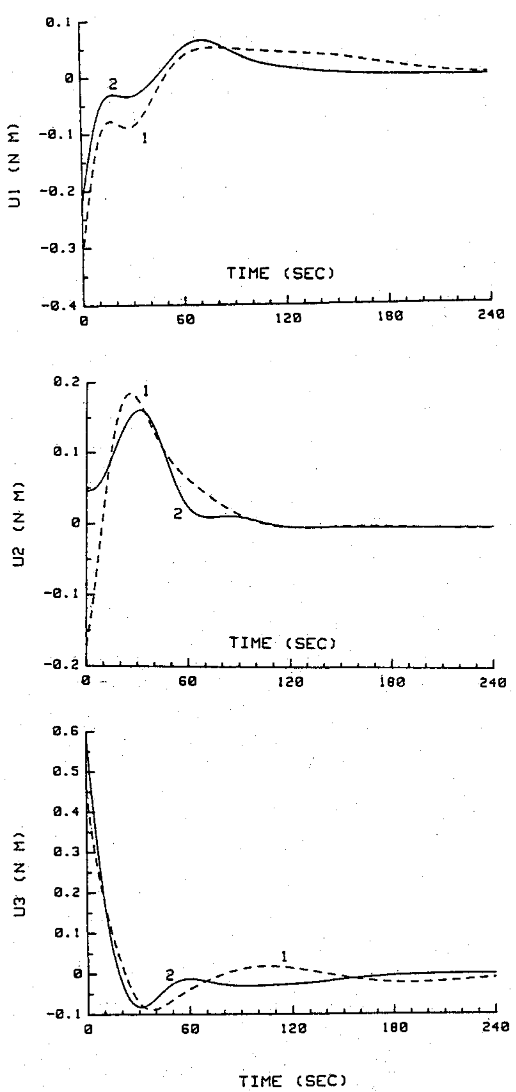

Fig. 7 Case 2: Control torques: 1, linear feedback; 2, linear plus quadratic feedback.

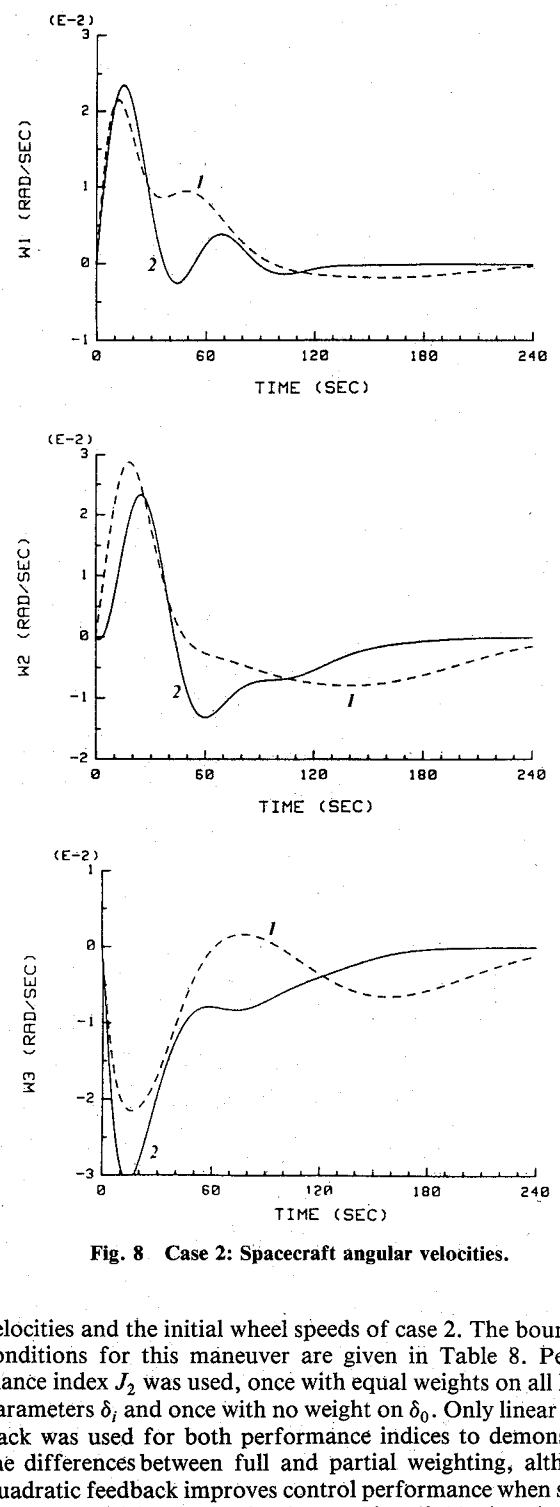

Fig. 8 Case 2: Spacecraft angular velocities.

which are evaluated at $t_f = 120$ s for the four-wheel maneuver and $t_f = 240$ s for the three-wheel maneuvers.

A comparison of performance indices with full and partial weighting on the Euler parameters is made. Q_1 indicates full state penalties in the performance index, and Q_2 implies that no penalties are put on δ_0. Figures 4 and 5 show the spacecraft and wheel angular velocities for the case of three orthogonal wheels (skew wheel off) and Q_2 in performance index J_2, which produced the lowest three-wheel performance index. The control torques are shown in Fig. 6.

Case 2

A rest-to-rest maneuver with nonzero initial wheel speeds is performed with three orthogonal wheels (skew wheel off) and no penalty on δ_0 in performance index J_2. This weighting produced the lowest performance index in cases 1 and 2. The boundary conditions are given in Table 6 and the performance indices evaluated at $t_f = 240$ s are given in Table 7. Since the initial and final Euler angles are the same as in case 1, the Euler parameters β_i are the same, but the system angular momentum is larger and, hence, the Euler parameters δ_i are different. Figures 7-9 plot the spacecraft and wheel angular velocities and control torques. Note that the final wheel speeds are 75, 50, and 100 rad/s for Ω_1, Ω_2, and Ω_3, respectively.

Case 3

A three-dimensional maneuver is demonstrated for the three-wheel configuration with large initial spacecraft angular velocities and the initial wheel speeds of case 2. The boundary conditions for this maneuver are given in Table 8. Performance index J_2 was used, once with equal weights on all Euler parameters δ_i and once with no weight on δ_0. Only linear feedback was used for both performance indices to demonstrate the differences between full and partial weighting, although quadratic feedback improves control performance when stable linear control is obtained. Figures 10 and 11 give the time histories of the Euler parameters, spacecraft angular velocities, and wheel speeds for these two cases.

Discussion

The performance indices in Tables 5 and 7 were reduced when quadratic feedback was added to the linear control. In both cases quadratic feedback produced Euler parameters that reached their final states earlier and resulted in a lower performance index. This also occurred with the spacecraft angular velocities in case 2.

A comparison was made between full and partial Euler parameter weighting in the performance index, since specifying values for three Euler parameters automatically produces a value for the fourth when the nonlinear state equations are used. No stability problems were encountered using partial

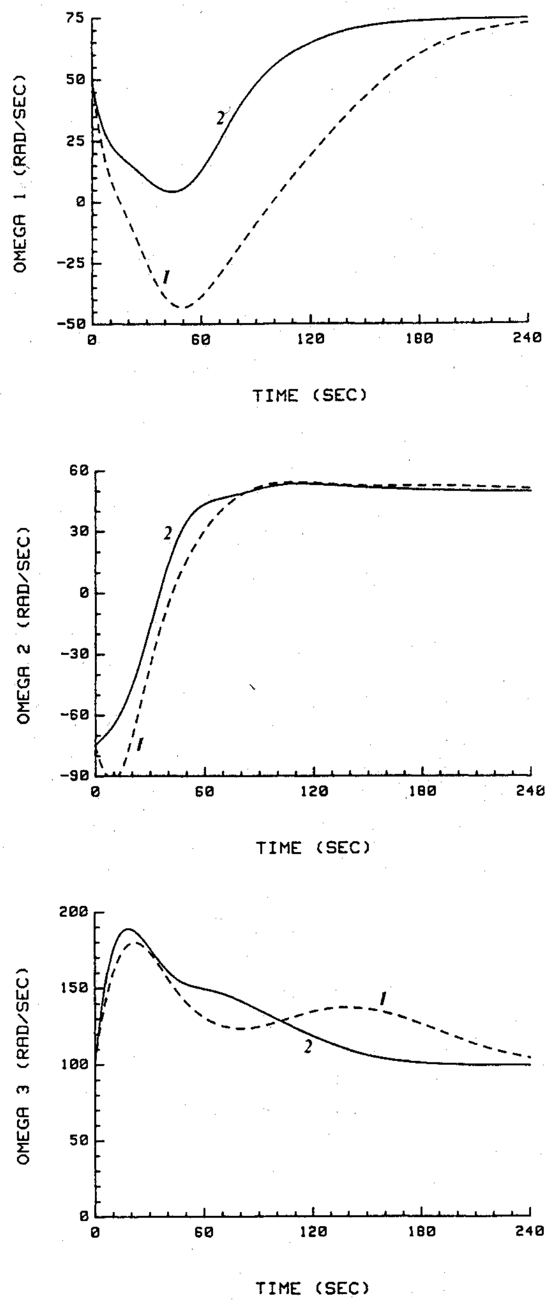

Fig. 9 Case 2: Wheel angular velocities: 1, linear feedback; 2, linear plus quadratic feedback.

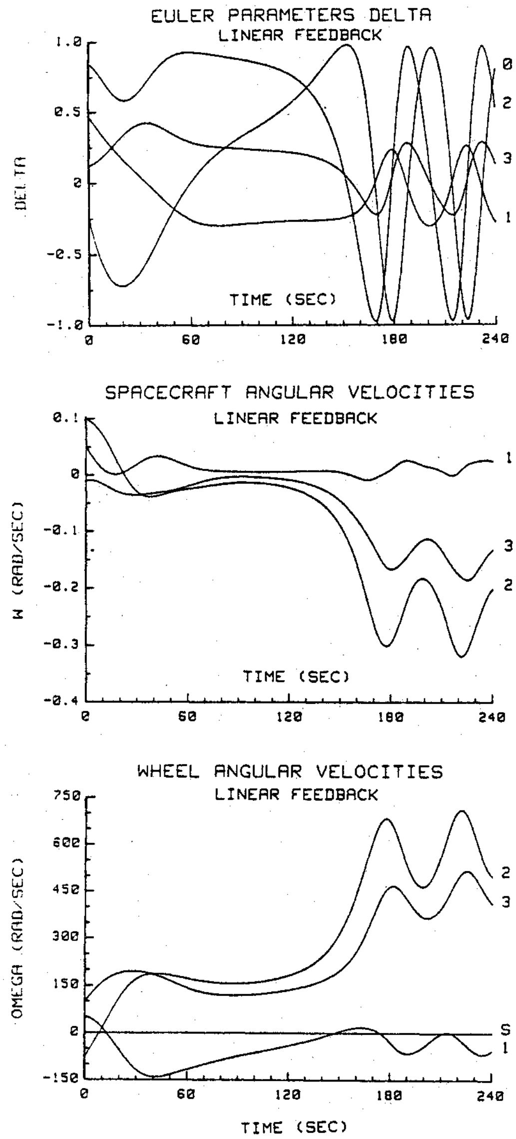

Fig. 10 Case 3: Unstable control.

Table 6 Case 2: Boundary conditions

	Initial states	Final states
ω_1	0.0	0.0
ω_2	0.0	0.0
ω_3	0.0	0.0
ϕ	$-\pi/2$	$\pi/2$
θ	$-\pi/3$	$\pi/3$
φ	$-\pi/4$	$\pi/4$
δ_0	−0.12815	0.37037
δ_1	0.59459	0.10026
δ_2	0.45281	0.74062
δ_3	0.65192	0.55159
Ω_1	50.0	—[a]
Ω_2	−75.0	—[a]
Ω_3	100.0	—[a]
Ω_4	0.0	—[a]

[a]See Table 4 footnote.

Table 7 Case 2: Performance indices

Linear feedback	4.81211
Linear plus quadratic feedback	4.29420

Table 8 Case 3: Boundary conditions

	Initial states	Final states
ω_1	0.0	0.0
ω_2	0.0	0.0
ω_3	−0.01	0.0
ϕ	$-\pi/2$	$\pi/2$
θ	$-\pi/3$	$\pi/3$
φ	$-\pi/4$	$\pi/4$
δ_0	−0.22769	−0.07728
δ_1	0.47213	−0.25249
δ_2	0.84335	0.93018
δ_3	0.11840	0.24472
Ω_1	50.0	—[a]
Ω_2	−75.0	—[a]
Ω_3	100.0	—[a]
Ω_4	0.0	—[a]

[a]See Table 4 footnote.

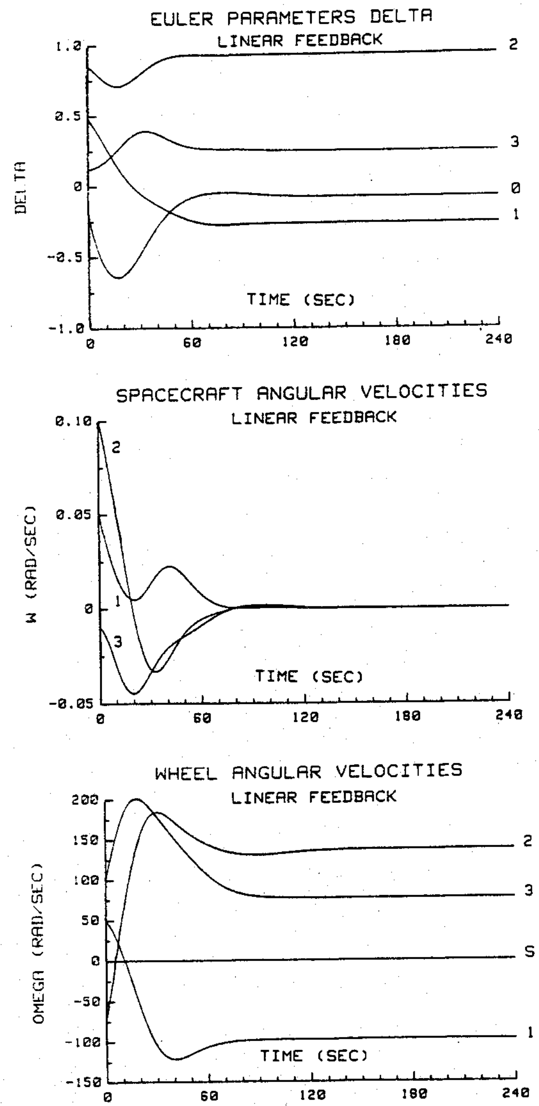

Fig. 11 Case 3: Stable control.

weighting as long as spacecraft velocities were small, but in case 3 partial weighting produced the tumbling behavior in Fig. 10. This unstable behavior occurs because the linear feedback gains are determined by only the linear parts of the state equations. Although the nonzero eigenvalues of $A-BR^{-1}B^TK$ have negative real parts, so that the linear closed-loop system is stable, the nonlinear terms in the state equations are large and produce unstable behavior in the simulation. Similar behavior is seen in cases 1 and 2, except that the quadratic terms in the state equations change δ_0 by a smaller perturbation that is not destabilizing.

When the departure motion of all four Euler parameters is penalized in the performance index, linear gains are determined that will keep δ_0 close to its desired final state. The quadratic terms in the state equations then do not produce destabilizing corrections to the linear closed-loop equations, since bounds have been placed on the states through the performance index. As is evident in comparing Figs. 10 and 11, introducing the penalty on δ_0 departure motion eliminates the tumbling motion and yields an attractive optimal maneuver.

Conclusions

Polynomial feedback on angular velocities and Euler parameters have been used for nonlinear control of a spacecraft with four reaction wheels. A comparison of linear and quadratic control was made, with a reduction in the performance index for quadratic feedback. When using redundant attitude variables, care must be taken so that the linear gains (based upon linearized departure motion state equations) result in modest violations of the implicit constraints. This may be enforced by penalizing all states in the performance index weight matrix.

Acknowledgments

The authors are pleased to acknowledge the constructive discussions of this work with Dr. S.R. Vadali. This work was supported by the Air Force Office of Scientific Research under Contract F4920-83-K-0032; the authors appreciate the support and capable technical liasion of Dr. Anthony K. Amos of AFOSR.

References

[1]Willenstein, A.P., "Optimal Regulation of Nonlinear Dynamical Systems on a Finite Interval," *SIAM Journal of Control and Optimization,* Vol. 15, Nov. 1977, pp. 1050-1069.

[2]Dabbous, T.E. and Ahmed, N.U., "Nonlinear Optimal Feedback Regulation of Satellite Angular Momenta," *IEEE Transactions on Aerospace and Electronic Systems,* Vol. AES-18, Jan. 1982, pp. 2-10.

[3]Dwyer, T.A.W. III and Sena, R.P., "Control of Spacecraft Slewing Maneuvers," *IEEE 21st Conference on Decision and Control,* Orlando, FL, Dec. 1982.

[4]Carrington, C.K. and Junkins, J.L., "Nonlinear Feedback Control of Spacecraft Slew Maneuvers," *Journal of the Astronautical Sciences,* Vol. 32, Jan.-March 1984, pp. 29-45.

[5]Potter, J.E., "Matrix Quadratic Solutions," *SIAM Journal of Applied Mathematics,* Vol. 14, May 1966, pp 496-501.

[6]Turner, J.D. and Chun, H.M., "Optimal Feedback Control of a Flexible Spacecraft During a Large-Angle Rotations Maneuver," AIAA Paper 82-1589, Aug. 1982.

[7]Juang, J.-N., Turner, J.D., and Chun, H.M., "Large-Angle Maneuvers of Flexible Spacecraft Using a Closed Form Solution for the Terminal Tracking Problem," AAS/AIAA Paper 83-375, Aug. 1983.

[8]Whittaker, E.T., "A Treatise on the Analytical Dynamics of Particles and Rigid Bodies," Dover Publications, New York, 1944, pp. 10-11.

[9]Vadali, S.R. and Junkins, J.L., "Spacecraft Large Angle Rotational Maneuvers with Optimal Momentum Transfer," *Journal of the Astronautical Sciences,* Vol. XXXI, April-June 1983, pp. 217-235.

[10]Kraige, L.G. and Junkins, J.L., "Perturbation Formulations for Satellite Attitude Dynamics," *Celestial Mechanics,* Vol. 13, 1976, pp. 39-64.

[11]Lee, E.B. and Markus, L., *Foundations of Optimal Control Theory,* John Wiley & Sons, New York, 1967.

[12]Kirk, D.E., *Optimal Control Theory,* Prentice-Hall, 1970.

[13]Hoffman, H.C., Donohue, J.H., and Datley, T.W., "SMM Attitude Control Recovery," AIAA Paper 81-1760, Aug. 1981.